Modeling the Kinetics of Sulfate Reduction and Sulfide Oxidation Involved in Treating Mining Wastewater Using the Membrane Biofilm Reactor (MBfR).

by

Gloria Appiah Nsiah

A Thesis Presented in Partial Fulfillment
of the Requirements for the Degree
Master of Science

Approved April 2021 by the
Graduate Supervisory Committee:

Bruce Rittmann, Chair
Peter Fox
Morteza Abbaszadegan

ARIZONA STATE UNIVERSITY

May 2021

ABSTRACT

The high levels of pollution associated with mining activities necessitates more efficient methods of treating mining effluent before it is released into the environment. Phosphate -mining wastewater contains high concentrations of sulfate that can be removed and recovered as elemental sulfur (S^0), which is a useful resource. The Membrane Biofilm Reactor (MBfR) uses gas-transfer membranes for the delivery of gases to microorganisms that carry out oxidation-reduction reactions that lead to the breakdown of contaminants. The two main microorganisms involved in the treatment of sulfate wastewater using the MBfR are sulfate-reducing bacteria (SRB) for the reduction of sulfate into sulfide and sulfur-oxidizing bacteria (SOB) for the oxidation of sulfide into S^0. In this work, the kinetic processes involved in sulfate reduction and sulfide oxidation for SRB and SOB were modeled using the steady-state biofilm model and mass balances on a completely mixed biofilm reactor. The model results identified trends of substrate removal, biofilm accumulation, and hydraulic retention time (HRT) for the design of sulfate-treatment system. The HRT required for 97.5% sulfate removal was about 0.1 d and that for 97.5% sulfide removal about 0.2 d. Higher levels of biofilm accumulation occurred with sulfide oxidation due to the larger biomass yield of the SOB. The needed delivery of H_2 gas required for sulfate reduction and O_2 gas for sulfide oxidation, as well as the alkalinity changes, also were determined based on the removal levels.

TABLE OF CONTENTS

Page

CHAPTER Page

LIST OF TABLES

Table Page

LIST OF FIGURES

Figure Page

1. INTRODUCTION

Overview

Most mining and mineral-processing industries, such as coal extraction, phosphate mining, and steel manufacturing, produce wastewater with high sulfate concentrations. When the wastewaters are released into natural waters, the high sulfate concentrations contribute to salinization of the freshwater, which may be harmful to the aquatic ecosystem (Runtti et al., 2018). Irrigation water taken from these sources may lead to white stains on plants and reduction in metabolic activities of cattle. In drinking water, no adverse effects of high sulfate concentrations have been found in adults. However, infants may respond to formulas with high sulfate concentrations by exhibiting symptoms of diarrhea. In addition, high sulfate in drinking water imparts unpleasant tastes (Moreno et al., 2009) and may cause release of metals from corrosion scales in pipes. The released sulfate also can be reduced under anaerobic conditions to hydrogen sulfide, which can be toxic in high concentrations and has an unpleasant "rotten egg" odor (Kinnunen, et al., 2017).

The effects of sulfate discharge into the environment necessitates efficient and cost-effective methods to treat mining wastewater. Among the good options is the Membrane Biofilm Reactor (MBfR), a fairly new technology that uses gas-transfer membranes to supply gaseous substrates to microorganisms responsible for the detoxification of contaminants and in water and wastewater. The hydrogen-based Membrane Biofilm Reactor (H_2-based MBfR) delivers hydrogen gas (H_2) as an electron donor and has the advantage of being able to reduce a wide range of oxidized contaminants (Chen et al.,

2017). MBfRs lower the cost of energy associated with gas bubbling, enhance gas utilization by the microorganisms, and provide high volumetric removal rates.

Biological removal of sulfate begins with the reduction of sulfate (SO_4^{2-}) to sulfide (S^{2-}). The sulfide then can be oxidized to elemental sulfur (S^0), which can be recovered for reuse (Pokorna & Zabranska, 2015). The microorganisms involved in the reduction pathway are sulfate-reducing bacteria (SRB), and sulfur-oxidizing bacteria (SOB) are involved in the oxidation pathway. These two groups of bacteria are distinct from each other in terms of genetics, physiology, and kinetics.

Problem Statement

My focus is on sulfate removal and sulfur recovery from phosphate-mining wastewater using the MBfR. My emphasis is on the biofilm kinetics for the SRB and SOB. I base the stoichiometry, kinetic parameters, and input parameters on the biochemistry and physiology of the SRB and SOB, along with the characteristics of phosphate-mining wastewater.

Organization

The following chapters are organized to provide background information, modeling methods, modeling results, and interpretations:

- Chapter two provides background information concerning pollution due to mining activities, specifically sulfate contamination in phosphate mining. The effects of mining effluent deposition on drinking water sources are discussed. Various

regulations and remediation activities currently being implemented are also discussed.

- Chapter three examines various sulfate-removal methods in use today, such as chemical and physical methods, but with emphasis on biological removal of sulfate. It also explores using the MBfR for sulfate removal. It addresses the MBfR configuration, its biochemical processes, and the ecological interactions among key microorganisms present in biofilm.
- Chapter four reviews the sulfate species present in the mining wastewater and the intermediate species of sulfate reduction. It outlines the sulfate-reduction and sulfide-oxidation pathways, including the biochemistry of the microorganisms involved are critically analyzed.
- Chapter five lays out the concepts and methods for modeling the biofilm kinetics of the bacteria involve in sulfate reduction and sulfide oxidation. The key parameters, input conditions, and equations necessary to analyze the two key bacterial types are developed in Chapter 5.
- Chapter six presents all the modeling results and interprets them in terms of challenges and opportunities when using the MBfR to treat phosphate-mining wastewater.
- Chapter seven provides a summary of thesis, implication of the research, and suggested areas for future consideration.

2. INDUSTRIAL MINING ACTIVITIES AND POLLUTION

Impact of Mining Activities

Mining of minerals is an industrial activity that has huge economic benefits and numerous health and environmental risks. On the economic side, many countries gain a large percentage of their economic activity from metal and non-metal ore mining. According to the National Mining Association of the USA (*A Report Prepared by the National Mining Association*, 2016), mining of coal, metallic ores, and non-metallic ores generates approximately 1.7 million jobs in the US and contributes about 220 billion US dollars to the Gross Domestic Product (GDP) and about 44 billion US dollars of taxes paid in 2015. On the environmental side, mining activities present health and environmental risks that include exposure of mined metals to the air, occupational hazards associated with the mining, pollution of agricultural soils, and pollution of aquatic ecosystems, including surface and groundwater sources of drinking water. (Duruibe et al., 2007).

Common Contaminants of Mining Processes

In most mining activities, one major contaminant is dust particles containing particulate metallic substances such as lead and arsenic (Csavina et al., 2011). Such toxic metals have well-known effects on the human respiratory health from long exposure and high levels (Ross & Murray, 2004). For example, high levels of cadmium were measured in the surrounding air of copper-smelting industries in Serbia (Serbula et al, 2017). Prolonged exposure resulted in lung, kidney, and cardiovascular problems. Agricultural soil sampled from around the Xiaohe Yelian smelting factory area in China contained

high levels of antimony (Sb), which caused changes in soil structure and vegetation types present in the area. (Sun et al., 2019). Uranium mining sites in the Northern Territory of Australia released radiological contaminants, as well as sulfate, magnesium, and manganese (Noller, 1991). At certain abandoned mining sites at southern Nevada, mercury and cyanide previously used in the extraction of gold and silver were detected decades after mine closure (Sims, 2011).

Effects of Mining Wastewater Discharges on Surface Water and Groundwater

One major effect of most mining activities is the discharge of contaminants to surface water and groundwater, which exposes drinking water sources and aquatic habitats to contamination by heavy metals and toxic compounds. In a study conducted to investigate the environmental impact of mining activities in the southern part of China (W. X. Liu et al., 2003), copper mines and smelting activities in the vicinity of the Lean River led to high levels of lead, copper, and zinc in the water and river sediments. The source was highly acidic (pH 2-3) wastewater effluent from the Denxing copper mine. Water sampled from the Mud River in West Virginia contained sulfate strontium isotopes as a result of the mountaintop coal exploration in the area (W. X. Liu et al., 2003). High concentrations of arsenic, cadmium, copper, and mercury were detected in feather and blood samples of Osprey birds that fed on fish in the Upper Clark Fork River in the area of a historical mining site in Montana, USA (Langner et al., 2012). At the coal mines at Gondwana, India, leachates containing high levels of sodium and sulfate were detected in the groundwater (Adhikari et al., 2013).

Various drinking-water sources sampled in small-scale gold-mining communities in the Northern part of Ghana contained high levels of mercury, lead, and arsenic, compared to maximum contaminant levels set by the World Health Organization (WHO); thus, the waters posed health risks to members of the community (Jonathan & Isaac, 2014).

The high levels of contaminants related to ore mining also may destroy the flora and fauna of water bodies, as observed in the above-mentioned scenarios of pollution due to mining. These environmental effects necessitate more efficient methods for treating wastewater before its release into the environment.

Regulation of Mining Activities and Remediation Processes

Due to the issues associated with mining pollution, many countries have specific guidelines for effluent emissions. Aspects of mining emissions that are regulated include particulate dust (Petavratzi et al., 2005), wastewater discharges, and mined-land remediation (EPA, 2016).

Various approaches have been applied in the remediation of pollution due to mining activities. Methods used for remediating soils contaminated by mine waste include washing using chemicals such as HCl, H_2SO_4, or Na_2EDTA (Moutsatsou et al., 2006).

One other approach is phytoremediation, which involves the use of specific species of plants, such as Crassulaceae and Brassicaceae, that are capable of bioconcentrating high levels of metals such as cobalt, cadmium, and arsenic, in their shoot system (Macklin et al., 2006) (Sun et al., 2019).

In polluted groundwater and surface waters, treatment and remediation may be done by the addition of wood shavings, limestone, and magnesia are to wastewater containing high concentrations of zinc, cadmium, magnesium, cobalt and nickel. This method has been applied in the management of acid mine drainage in sulfide mining areas, such as the Iberian Pyrite Belt in Europe.

Papirio et al. (2013) reviewed other remediation options for acid mine drainage, such aerobic and anaerobic wetlands, *ex situ* reactors, and *in situ* reactive barriers. In Bitterfeld, Germany, the spread of pollution to groundwater and surface water has been mitigated by *ex situ* "pump and treat" methods (Wycisk et al., 2003). Another method commonly used is the treatment of the mining effluents by its addition to conventional wastewater treatment systems (Wang et al., 2005).

Phosphate Mining and Sulfate Contamination

Uses of phosphate minerals

Phosphate is mined for its numerous beneficial uses. The most significant use of phosphate is in agriculture as part of fertilizers, since phosphate is an essential mineral in plant growth (Dissanayake & Chandrajith, 2009). About 90% of mined phosphate goes to fertilizer production today (Gurr, 2018). Other uses of phosphate include the manufacturing of construction materials, such as cements, and in the manufacturing of certain food products, such as soft drinks (Zhang, 2014).

Major phosphate-mining activities in the world

The abundance of phosphorus in the earth crust is about 0.12%, mainly in the form of apatite $Ca_5(PO_4)_3$ (Sutphin et al., 1990). The countries with the major phosphate deposits are Morocco, China, Syria, and the United States (DeYoung et al., 1984) (Orris & Chernoff, 2004). Morocco is the leading phosphate-mining country, and it supplies around 75% of phosphate ore today (Mar & Okazaki, 2012).

Phosphate mining and ore processing

The phosphate mining process involves the excavation of the metal ore from phosphate reserves. The ore is then washed and processed using sulfuric acid to extract phosphate (Mendes et al., 2020). Other chemicals, such as ammonium for fertilizer production, may be added (Ellis & Hanlon, 2013).

Ore processing with sulfuric acid produces phosphogypsum ($CaSO_4.nH_2O$) as a by-product (Tayibi et al., 2009). About 4 tons of phosphogypsum are produced for every ton of fertilizer manufactured from phosphate (Ellis & Hanlon, 2013). Phosphogypsum has a high concentration of sulfate, which poses management challenges. However, mining industries can retrieve the sulfate and convert into elemental sulfur (S^0) (de Beer et al., 2015), which can be used for producing sulfuric acid (Apodaca et al., 2017), reducing the cost of production while also mitigating the effect of high sulfate release into the environment.

Other chemical components typically found in phosphate-mining effluents include chlorine, fluoride, iron, and low concentrations of zinc, copper, cadmium, and manganese

(Chraiti et al., 2016), (G. L. Reta et al., 2019). Phosphate mining ores also may contain radioactive elements such as uranium and thorium (Zhang, 2014).

Concerns about phosphate mining

The major concerns of phosphate mining in relation to water quality are effluent discharges into surface water and groundwater, air pollution, and the impact on land use. The phosphogypsum produced contains toxic heavy metals that may result in the pollution of groundwater and aquatic environments (Motalane & Strydom, 2004). One other major problem is the presence of radioactive elements such as radium and radon gas in the phosphogypsum produced (Attallah et al., 2019), which poses risks on public health (Othman & Al-Masri, 2007). The effect on land use includes soil erosion, clearing of vegetation during mining and leachate into agricultural soils (Martinez-Escobar & Mallela, 2019).

Concerning water quality, the sulfate, fluoride and sodium ions released through discharge increases their levels of surface water and groundwater sources. The acidity of the mine effluents also may have a negatively impact on the biosphere of surface waters (G. Reta et al., 2018).

3. SULFATE CONTAMINATION AND REMOVAL METHODS

Impacts of Sulfate Discharges on the Environment

Sulfate discharges in the environment alter the natural sulfur cycle, resulting in the buildup of sediments rich in sulfate in seas and other water bodies. The accumulated sulfates may be reduced to sulfide, causing sulfide toxicity in the environment (Lens et al., 1998).

Another impact of high sulfate concentration is in distribution systems and wastewater sewers: corrosion by the formation of hydrogen sulfide (H_2S) that is subsequently oxidized to sulfuric acid. The H_2S produces toxicity and bad odors (Tait et al., 2009); the formation of sulfuric acid leads to corrosion (Nnadi & Lizarazo-Marriaga, 2013). Similarly, a high sulfate concentration can reduce the durability of cementitious concrete used in construction processes (H. Liu et al., 2017).

Sulfate toxicity to methane-producing microorganisms may occur in anaerobic digestion of sludge. Also, sulfate reduction reduces methane production by competing or organic electron donors. Furthermore, H_2S is a harmful biogas contaminant (Khanal & Huang, 2005).

Sulfate Regulation

Various discharge limits for sulfate concentrations have been set in most countries. Sulfate discharge limits for mine effluents typically range between 250-1000 mg/L, while the typical concentration in mining wastewater may be up to 10,000 mg/L (Runtti et al., 2018). Currently, the US EPA has no set maximum contaminant level (MCL) for sulfate

in drinking water. However, a secondary standard of 250 mg/L has been set for aesthetic reasons (to prevent undesirable tastes caused by high levels of sulfate) ((US EPA), 2017).

Sulfate-removal Processes

Treatment processes that are used for sulfate removal include chemical treatment, biological removal, and certain integrated processes. (Kinnunen, et al., 2017).

Chemical and physicochemical removal methods

Sulfate in water can be removed by the addition of chemicals such as $Ba(OH)_2$, which precipitates with sulfate in the form $BaSO_{4(s)}$ (Bologo et al., 2012). Lead (Pb^{2+}) and calcium (Ca^{2+}) ions also can be added to precipitate sulfate as $PbSO_{4(s)}$ or $CaSO_{4(s)}$ respectively, which can be removed by centrifugation or filtration (Benatti et al., 2009). A similar process is crystallization (Tait et al., 2009), which also involves the addition of chemicals such aluminum to form gypsum crystals.

Ion exchange is physiochemical process that involves, for example, the exchange of the sulfate anion for the hydroxyl ion (Darbi et al., 2003). Electrodialysis and reverse osmosis are membrane processes that can be used in sulfate removal (Chao & Liang, 2008).

Even though chemical and physicochemical processes are widely used for sulfate removal, they have disadvantages of high cost of chemicals, low removal efficiency, and production of large amounts of sludge (Oztemur et al., 2020).

Biological removal methods

Biological sulfate removal involves microorganisms, mainly sulfate-reducing bacteria, in the presence of an electron donor, to reduce sulfate to sulfide. Various methods of biological sulfate removal and the microorganisms involved are further expounded in the following chapters.

Integrated processes

Certain integrated processes combine an electrochemical process and a biological process. For example, sulfate-reducing bacteria reduce sulfate to sulfide, after which the sulfide is electrochemically oxidized to elemental sulfur (Liang et al., 2013).

4. BIOLOGICAL SULFATE REMOVAL

Methods of Biological Removal of Sulfate

Several reactor configurations have been used in the biological treatment of sulfate in industrial wastewater. All provide a favorable environment for the growth of microorganisms by delivering necessary electron-donor substrate and retaining the biomass. A few of the reactor configurations are discussed below.

Fluidized bed reactors pass the wastewater through a medium of suspended particles, such as activated carbon or anthracite, with a fluid velocity just enough to keep the particles suspended. The sulfate-containing wastewater come into contact with the sulfate-reducing microorganisms that are retained in a biofilm of the fluidized particles. An organic electron donor, such as lactate or ethanol (Kaksonen et al., 2003), is added to the influent. This configuration has the advantages of good biomass retention, prevention of clogging, and high removal rates per unit volume. Disadvantages can include problems maintaining stable bed fluidization, pumping costs, and methanogenesis (Zitomer & Shrout, 2000).

The upflow anaerobic sludge blanket (UASB) has a similar mode of operation as fluidized beds, but the suspended biofilm carriers are self-forming (Arne Alphenaar et al., 1993). Baffled reactors, a variation on the UASB, are used in biological sulfate removal (Zitomer & Shrout, 2000). Baffles direct the wastewater upward and downward through a series of connected chambers with sludge blankets, which retains the biomass in the system (Rittmann & Mccarty, 2000).

Packed-bed reactors are usually cylindrical tubes filled with pellets made of materials such as rocks, zeolites, or plastic carriers. The wastewater is passed through the bed, and the pellets serve as surfaces for biomass growth. Packed-bed reactors are known to be cost efficient in terms of operation and maintenance and also easy to operate. However, major problems with their operation are issues bed clogging, short-circuiting, and temperature control (Silva et al., 2002) (Catalano S, 2018).

Membranes are used to enhance biomass retention. Sulfate-reduction reactors with membranes include the fluidized-bed membrane bioreactor, which is a modification of the fluidized bed bioreactor (Oztemur et al., 2020), and the membrane biofilm reactor (MBfR), which is further expanded in the next chapter of this paper.

Microorganisms Involved in Sulfate Removal

Sulfate reducing-bacteria (SRB)

SRB comprise a phylogenetically diverse group of prokaryotes capable of utilizing sulfate as an electron acceptor in respiration. They are strict anaerobes (Dolla et al., 2006) known to be metabolically versatile, although certain species are capable of reducing other electron acceptors, such as nitrate, in the absence of sulfate (Sousa et al., 2017). SRB utilize a wide range of electron donors, such as hydrogen, methane, ethanol methanol, and lactate (Liamleam & Annachhatre, 2007). Organic donors used for SRB include lactate, pyruvate, and alcohols such as butanol, propanol and ethanol (Gibson, 1990). SRB also can be involved in respirations of selenite, uranium, iron, mercury, and chromium. They are applied in biotechnology for wastewater treatment, control of

biocorrosion, fuel production, and bioremediation (Barton, 1995). SRB also can be involved in ulcerative colitis in humans (Rowan et al., 2009).

One of the main genera of SRB is the gram-negative *Desulfovibrio,* with species including *D. profundus, D. desulfuricans* and *D. simplex.* They are known to be capable of reducing nitrate as an electron acceptor in the absence of sulfate (Sousa et al., 2017).

Generally, SRB exhibit an optimum growth rate at pH between 6-8 and temperature of 15-45˚C (Haouari et al., 2006), (Kikot et al., 2010).

Sulfide-oxidizing Bacteria (SOB)

SOB utilize oxygen (O_2) as an electron acceptor and hydrogen sulfide (F. F. Xia et al., 2014) or thiosulfate as the electron donor (Fischer et al., 2015). Most common genera of SOB include *Thiobacillus Pseudomonas* and *Halothiobacillus*. Certain species of SOB also are capable of reducing nitrate or nitrite as an electron acceptor, including *Thiobacillus denitrificans* and *Paracoccus denitrificans* (Hutt, 2017). SOB generally have optimum conditions of pH ranging between 6-10 and temperature between 4-40˚C (Hutt, 2017) (Hidayat et al., 2017).

Other Microorganisms

In anaerobic biofilm systems, other microorganisms, such as methanogens and homoacetogens and nitrate reducers, may be present and may compete with SRB for substrates (A. Ontiveros-Valencia et al., 2018) (Meulepas et al., 2010). SRB are capable of outcompeting methanogens for H_2 when sufficient sulfate is present, such as in mining wastewater, due to a higher affinity of SRB for hydrogen than methanogens (Dar et al.,

2008). Homoacetogens also generate acetate which could be an electron donor for SRB, even though they also compete with SRB for H_2.

The sulfur-recovery Process

The stable forms of sulfur are sulfate SO_4^{2-} (+6 oxidation state), sulfide S^{2-} (-2 oxidation state), and elemental sulfur S^0 (0 oxidation state). Sulfate is the most oxidized sulfur species in the environment (Schwarz et al., 2020) and the most thermodynamically stable form of sulfur in aerobic conditions. In anaerobic conditions, hydrogen sulfide is the most stable form. (Barton & Fauque, 2009). Other sulfur species that may be found in the environment and in industrial wastewater effluents are sulfite, dithionate, and thiosulfate (Liamleam & Annachhatre, 2007).

In the treatment of sulfate-rich wastewater, sulfate is first converted into sulfide. The sulfide can then be converted into elemental sulfur for recovery. Elemental sulfur can be reused for the production of sulfuric acid used in the processing of mine ores (Zhao et al., 2017). They are also useful in processes such as bioleaching copper-containing electronic wastes (Hong & Valix, 2014). Sulfur may be oxidized back into sulfates, forming a cycle as represented in Figure 1.

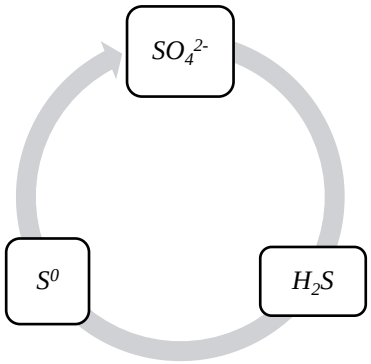

Figure 1 - Simplified sulfur cycle showing the main sulfur species involved in the treatment of sulfate wastewater.

Reduction of sulfate to sulfide

Sulfate-reducing bacteria (SRB) carry out biological sulfate reduction to sulfide using a wide range of electron donors, such as hydrogen, methanol, formate, acetate, and ethanol. Using hydrogen (H_2) as electron donor, the energy-generating reaction is (Schwarz et al., 2020):

$$4H_2 + SO_4^{2-} + H^+ \rightarrow HS^- + 4H_2O \qquad \Delta G = -151.9\ kJ/reaction \qquad (1)$$

This overall reaction involves two major steps: the reduction of sulfate (SO_4^{2-}) to sulfite (SO_3^{2-}) and the reduction of SO_3^{2-} to sulfide (S^{2-}) (Qian et al., 2019a). *Desulfovibrio* species are known to be the sulfate-reducing species that are cultured most easily and quickly (Barton & Fauque, 2009). They have, therefore, been used in the investigation of sulfate reduction by SRB.

Reduction of sulfate to sulfite by Desulfovibrio

In the reduction of sulfate to sulfite, sulfate is first activated to adenylyl sulfate (APS) using ATP by the enzyme ATP sulfurylase, forming inorganic pyrophosphate (PPi). The reactions are shown in equations 2-4.

$$SO_4^{2-} + ATP + 2H^+ \rightarrow APS + PPi \qquad \Delta G^{o'} = +46 kJ/mol \qquad (2)$$

Since the formation of PPi is not thermodynamically favorable, a second enzyme (inorganic pyrophosphate phosphohydrolase) hydrolyzes PPi:

$$PPi + H_2O \rightarrow 2Pi \qquad \Delta G^{o'} = -22\ kJ/mol \qquad (3)$$

Next, APS is reduced to bisulfite and AMP by the APS reductase enzyme (Barton & Fauque, 2009):

$$APS + H_2 \rightarrow HSO_3^- + AMP + H^+ \quad \Delta G^{o'} = -69\ kJ/mol \qquad (4)$$

Equations 2-4 can be summarized as:

$$SO_4^{2-} + 2ATP + H^+ + H_2 + H_2O \rightarrow HSO_3^- + 2ADP + 2Pi \qquad \Delta G^{o'} = -45\ kJ/mol \quad (5)$$

Reduction of sulfite to sulfide

The reduction of sulfide to sulfite is catalyzed by the enzyme sulfite reductase. Using hydrogen as the electron donor, the reaction yields a standard free energy of -174 kJ/mol and additional ATP (Santos et al., 2015). The overall reaction is known to occur in three steps known as the trithionate pathway, shown by equations 7-9.

First, the reduction of sulfite to trithionate:

$$1.5HSO_3^- + 1.5SO_3^{2-} + H_2 + 2.5H^+ \rightarrow S_3O_6^{2-} + 3H_2O \quad \Delta G^{o'} = -48\ kJ/mol \qquad (7)$$

Next, the reduction of trithionate to thiosulfate with sulfite:

$$S_3O_6^{2-} + H_2 \rightarrow S_2O_3^{2} + 0.5SO_3^{2-} + 0.5HSO_3^- + 1.5H^+ \quad \Delta G^{o'} = -122\ kJ/mol \qquad (8)$$

Finally, the reduction of thiosulfate to sulfite and sulfide:

$$S_2O_3^{2} + H_2 \rightarrow 0.5HS^- + 0.5H_2S + 0.5HSO_3^- + 0.5SO_3^{2-} \qquad \Delta G^{o'} = -4\ kJ/mol \qquad (9)$$

Figure 2 presents a summary of the intermediate species involved in the reduction of sulfate to sulfide. The production of hydrogen sulfide (H_2S) is unwanted due to its toxicity in the environment and to certain aerobic microorganisms (Gibson, 1990).

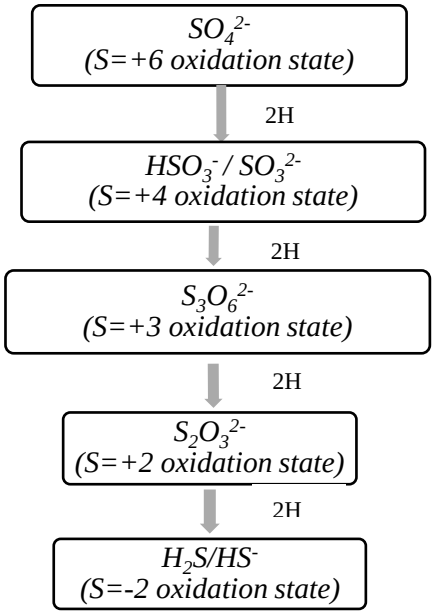

Figure 2-The various intermediate species in the reduction of sulfate to sulfide

Oxidation of sulfide to elemental sulfur

Using O_2 as an electron acceptor, SOB carry out the oxidation of hydrogen sulfide into sulfate according to:

$$H_2S + 2O_2 \rightarrow SO_4^{2-} + 2H^+ \quad \Delta G^{o'} = -796.56 kJ/mol \qquad (10)$$

or into elemental sulfur according to the reaction as shown by equation 11:

$$H_2S + 2O_2 \rightarrow 2S^0 + 2H_2O \quad \Delta G^{o'} = -209.34\ kJ/mol \qquad (11)$$

which is preferred in this situation. To favor the oxidation of sulfide to elemental sulfur, the key factor is the regulation of the sulfide to oxygen ratio (De Gusseme et al., 2009).

The Membrane Biofilm Reactor for Sulfate Removal

The MBfR process

Biofilms are an aggregation of microorganisms forming a community that is held together on a surface by extracellular polymeric substances (EPS) (Horn & Lackner, 2014). This offers the microorganisms resilience against being washed out and the ability to survive harmful environmental conditions. The diversity of biofilms may enable the availability of substrates to one group of microorganisms due to the metabolic activities of another. However, it may also result in competition for nutrients among the groups of microorganisms desirable or not desired for the performance goals of the system. The key microorganisms present in biofilms for sulfate removal are addressed in subsequent sections.

The MBfR uses gas-transfer membranes as a substratum for biofilm growth and retention, as well as for the delivery of a gaseous substrate. The H_2-MBfRR delivers H_2 as an electron donor used by microorganisms for the reduction of a large number of contaminants (Zhou et al., 2019). O_2 gas is delivered in the O_2-MBfR as an electron acceptor for the oxidation of certain organic substrates, such as benzene and toluene (Z. Liu et al., 2018). Other gases that can be delivered by the MBfR for contaminants removal are carbon dioxide (CO_2), methane (CH_4), and ammonia (NH_3) (Rittmann, 2011).

One advantage of the H_2-MBfR is its ability to reduce multiple contaminants in water at the same time. These include the reduction of perchlorate (ClO_4^-) to chlorine iron (Cl^-) (Aura Ontiveros-Valencia et al., 2014), nitrate (NO^-_3) and nitrite (NO^-_2) to N_2 gas (denitrification) (Tang et al., 2013), selenate (SeO_4^{2-}) and selenite (SeO_3^{2-}) to solid selenium (Se^o) (Zhou et al., 2019), and certain organic contaminants such as endosulfan (Cuci & Taşkın, 2020), trichloroethane (TCE), and tetrachloroethane (PCE) (Karataş et al., 2014) into benign forms such as Cl^-, C_2H_6, or C_2H_4.

Another advantage is that the MBfR allows for almost 100%-efficient H_2 delivery and precise control of the H_2-delivery capacity (Zhou et al., 2019; Schwarz et al., 2020).

The MBfR configuration and setup for sulfate removal

The MBfR is able to deliver H_2 as electron donor and CO_2 as a carbon source to SRB for sulfate reduction, and O_2 as electron acceptor to SOB for sulfide oxidation. Figure 3 is an illustration (Schwarz et al., 2020) of the MBfR for the removal of sulfate in mining

wastewater. The sulfate-rich wastewater is fed into the H_2-based MBfR and CO_2 is delivered for sulfate (SO_4^{2-}) reduction into sulfide (H_2S, HS^-) by SRB. The effluent of the H_2-based MBfR is then fed into the O_2-based MBfR for the conversion of the sulfide into elementary sulfur (S^0) by SOB, and then directed to the effluent. CO_2 is delivered into the systems as an inorganic carbon source for the autotrophic bacteria either by simultaneous delivery with the gases (H_2/O_2) or by gas sparging (S. Xia et al., 2016).

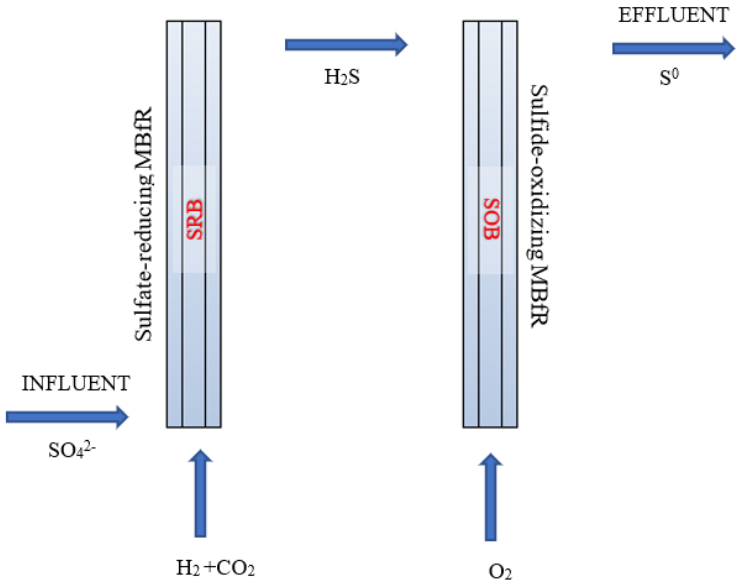

Figure 3-An illustration of the MBfR set up for sulfate conversion into elemental sulfur.

The MBfR is made of bundles of hollow-fiber membranes (non-porous) that are connected to a gas supply. Figure 4 shows a laboratory-scale MBfR setup for sulfate reduction. The membrane fibers are bundled in a tube into which the influent feed is directed and connected to a gas supply that delivers gases for the growth of biofilms on the membranes. Pipes are then connected to the tubes to the effluent for sampling.

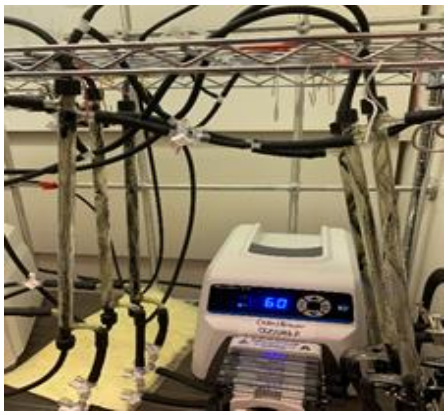

Figure 4-A bench scale set up of the MBfR showing bundles of fibers connected to a gas supply. Credits: Anwar Alsanea, BSCEB.

5. MATHEMATICAL MODELING

Engineering modeling involves the implementation of fundamental concepts to describe or predict the performance of a real engineering system. Modeling is an integral element of environmental engineering for making analysis and design of environmental processes. A biofilm model is a mathematical representation of substrate utilization, biomass growth and loss, substrate mass transport in a biofilm system.

In terms of complexity, a biofilm model can be one-dimensional, two-dimensional, or three-dimensional (Wanner et al., 2006). It may have a solution that is analytical (the simplest model with many assumptions, such as first-order reaction kinetics and a fixed amount of biofilm), pseudo-analytical (a less simple form in which the number of assumptions is reduced), or numerical (a more complex model involving numerical techniques and may include a multispecies system with changing conditions). A model's rate expressions can also be linear or nonlinear (that is, the relationship between quantities may exhibit a constant or variable rate of change) and involve steady or non-steady state conditions (D'Acunto et al., 2019). Simple models have been known to work well to represent systems and are therefore selected to remove the need for complexity in designs. However, more complex models may be employed depending on the desired precision and accuracy goals and the type of data available (Araghinejad, 2014).

A relatively simple, pseudo-analytical model is applied in this work. The processes are analyzed for steady-state conditions, which assumes that the biomass per unit surface area throughout the biofilm and the substrate utilization rate are constant with time.

Modeling of Biofilm Processes

I modeled each of the two processes (sulfate reduction and sulfide oxidation) as occurring in a Completely Mixed Biofilm Reactor (CMBR), represented by the diagram in Figure 5. Key characteristics of the CMBR are:

a. The influent substrate concentration in flow Q (m^3/d) is S^0 (g O_2 eq/L), where O_2 eq (also OE) stands for oxygen (O_2) equivalents, that is 8 g O_2 per electron equivalent.
b. The effluent substrate concentration is equal to the substrate concentration in the reactor S (g O_2 eq/L).
c. All microbial reactions occur in the biofilm, which has a specific surface area a (m^{-1}). The total surface area (m^2) is thus given as aV, where V is the reactor volume (m^3).
d. The biofilm accumulation per surface area (g VS/m^2, where VS stands for biomass as volatile solids) is $X_f L_f$, where X_f is the biofilm's biomass density (g VS/m^3) and L_f is the biofilm's thickness (m); thus, the total biofilm accumulation (g VS) is given as $X_f L_f aV$.

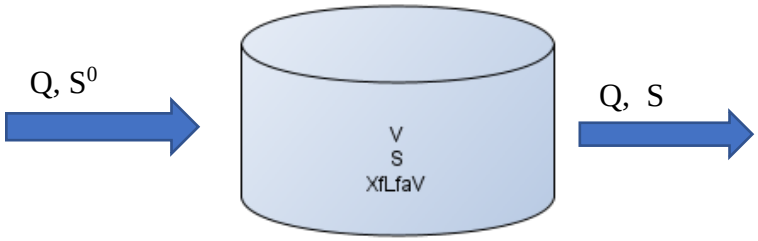

Figure 5-A representation of a CMBR and its characteristics.

Input Parameters and Equations

Estimating energetics and biomass yield

In order for microorganisms to gain energy for growth and cell maintenance, they carry out oxidation-reduction reactions that involve an electron donor and an electron acceptor. A portion of the electron donor (f_e^o) is transferred to the electron acceptor to generate energy which is used to convert the rest of the electron donor (f_s^o) into new cells.

For sulfate reduction by SRB, the electron acceptor is sulfate (SO_4^{2-}) and the electron donor selected in this work is hydrogen gas (H_2). For sulfide oxidation by SOB, the electron donor is sulfide (S^{2-}), and the electron acceptor is oxygen (O_2). Sulfate is taken as the rate-limiting substrate for the growth of SRB, and it is sulfide for the SOB. Thus, ig is assumed that the delivered gases (O_2 and H_2) are not rate-limiting. This assumption means that competition for the delivered gases by other microorganisms in the system is not occurring and that growth of the microorganisms is dependent on the concentrations of sulfate (for SRB) and sulfide (for SOB). However, careful delivery of the gases to minimize loss of either gas could lead to some rate limitation by the delivered gas. This situation might cause the kinetics to be slower than presented here.

Equations 12 to 17 present the electron donor and electron acceptor half reactions and overall energy reactions involved in sulfate reduction and sulfide oxidation and the free energies at pH = 7.

<u>Sulfate reduction by SRB</u>

The electron-acceptor half reaction is

$$\frac{1}{8}SO_4^{2-} + \frac{5}{4}H^+ + e^- \rightarrow \frac{1}{8}H_2S + \frac{1}{2}H_2O \qquad \Delta G^{o'} = +20.9\ kJ/e^-\ eq \qquad (12)$$

The electron-donor half reaction is

$$\frac{1}{2}H_2 \rightarrow H^+ + e^- \qquad \Delta G^{o'} = -39.87\ kJ/e^-\ eq \qquad (13)$$

The combined overall energy equation is

$$\frac{1}{8}SO_4^{2-} + \frac{1}{2}H_2 + \frac{1}{4}H^+ \rightarrow \frac{1}{8}H_2S + \frac{1}{2}H_2O \qquad \Delta G^{o'} = -18.97\ kJ/e^-\ eq \qquad (14)$$

Sulfide oxidation by SOB

The electron-acceptor half reaction is

$$\frac{1}{4}O_2 + H^+ + e^- \rightarrow \frac{1}{2}H_2O \qquad \Delta G^{o'} = -78.72\ kJ/e^-\ eq \qquad (15)$$

The electron-donor half reaction is

$$\frac{1}{2}H_2S \rightarrow \frac{1}{2}S^0 + e^- + H^+ \qquad \Delta G^{o'} = -24.9\ kJ/e^-\ eq \qquad (16)$$

The combined overall energy equation is (Sahinkaya et al., 2011)

$$H_2S + \frac{1}{2}O_2 \rightarrow S^0 + H_2O \qquad \Delta G^{o'} = -103.67\ kJ/e^-\ eq \qquad (17)$$

(Rittmann and McCarty, 2020).

The sulfide-oxidation process yields a higher overall energy, compared to the sulfate-reduction process. This difference directly affects the yield and biomass growth rates of the two groups of bacteria, as is shown in subsequent sections.

Estimation of Microbial Parameters

Calculating the true yield of (Y) and the maximum specific growth rate of bacteria (μ_{max})

The true yield (Y) quantifies the portion of donor electrons converted to biomass during cell synthesis and respiration. It is directly related to the energy yield of the energy reaction and the energy cost of synthesis. The maximum specific growth rate of bacteria (μ_{max}) is the rate of increase of bacteria cells per unit biomass concentration. μ_{max} is used with Y to estimate the minimum concentration of substrate needed to support bacteria growth (S_{min}).

In order to calculate Y and μ_{max}, the equivalent donor used for energy production per equivalent of cells formed (A) is first calculated and used to determine f_e^o and fs^o, which are, respectively, the portion of electron donor transferred to electron acceptor for energy and the portion used for biomass synthesis.

Rittmann & McCarty (2020) present equations for arriving at the calculation of Y and μ_{max} using the energy associated with the conversion of carbon source to organic intermediates (ΔG_p) and the energy associated with the nitrogen source for cell synthesis (ΔG_{pc}). For the reactions under consideration, the carbon source is CO_2, and the nitrogen source is NH_4^+.

The energy required for cell synthesis (ΔG_s) is calculated using:

$$\Delta G_s = \frac{\Delta G_p}{\varepsilon^n} + \frac{\Delta G_{pc}}{\varepsilon} \qquad (18)$$

in which where ε is the efficiency coefficient accounting for energy loss due to electron transfer to synthesis. From table 1, ΔG_r is the free energy per electron equivalent of donor oxidized according to the energy reaction. The n exponent is either +1 or -1 for a positive ΔG_p or negative ΔG_p, respectively. q_{max} is the maximum specific rate of utilization of electron donor, Mc (113gcells/mol cells) is the molecular weight of cells represented as $C_5H_7O_2N$, and n_e (20 e^- eq/mol cells) is the number of electron equivalents per mole of cells.

The equivalent donor used for energy production per equivalent of cells formed (A) can be calculated, from which f_s^o, f_e^o, Y, and μ_{max} can be obtained (Rittmann and McCarty, 2020). Table 1 shows the equations and the calculated values for the parameters for sulfate reduction and sulfide oxidation.

Table 1-Values of microbial parameters for SRB and SOB

REACTION	A (e^- eq_S/ e^- eq_{ED})	f_s^o (e^- eq_X/ e^- eq_{ED})	f_e^o (e^- eq_{EA}/ e^- eq_{ED})	Y (g O_2 eq_x/ g O_2 eq_{EA})	q_{max} (g O_2 eq_{ED}/ g O_2 eq_X.d)	μ_{max} (1/d)
EQN.	$-\frac{\Delta G_s}{\varepsilon \Delta G_r}$	$\frac{1}{1+A}$	$1 - fs^o$	$\frac{fs^o}{fe^o}$	$\frac{8}{fe^o} * \frac{1}{1.42 \frac{g\ O_2\ eq_x}{gVSS}}$	Y $*$ q_{max}
$SO^{2-}_4 \rightarrow S^{2-}$ by SRB	18.8	0.054	0.949	0.054	5.6	0.303
$S^{2-} \rightarrow S^0$ by SOB	3.41	0.3	0.77	0.3	7.32	2.2

A large difference is observed in the f_s^0, Y, and μ_{max} values for SRB versus SOB. A larger proportion of electron donor is used for the formation of SOB in sulfide-oxidizing than for SRB in sulfate reduction. Therefore, higher rate of cell growth and a higher utilization of substrate occur for SOB.

From the calculated values of f_s^0 and f_e^0, the overall reaction for the two processes can be determined as shown in equation 19.

Overall reaction = $f_e^0(R_a) + f_s^0(R_c) - R_d$ *(19)*

where R_a is the acceptor half-reaction, R_d is the donor half-reaction, and R_c is the cell-synthesis half reaction. The cell-synthesis half reaction when NH_4^+ is the nitrogen source is

$$\frac{1}{5}CO_2 + \frac{1}{20}HCO_3^- + \frac{1}{20}NH_4^+ + H^+ + e^- \rightarrow \frac{1}{20}C_5H_7O_2N + \frac{9}{20}H_2O \quad (20)$$

Using equations 13, 14, 19, and 20, as well as the parameter values in Table 1, the overall reaction for sulfate reduction to sulfide is

$$\frac{1}{2}H_2 + 0.12SO_4^{2-} + 0.0125CO_2 + 0.0025NH_4^+ + 0.2375H^+ \rightarrow 0.12H_2S + 0.0025C_5H_7O_2N + 0.5H_2O \quad (21)$$

Similarly, the overall reaction for sulfide oxidation to elemental sulfur can be derived using equations 15, 16, 19, and 20, along with Table 1:

$$\frac{1}{2}H_2\mathrm{S} + 0.19O_2 + 0.07\mathrm{C}O_2 + 0.0115\mathrm{N}H_4^+ \rightarrow \frac{1}{2}S^0 + 0.0115C_5H_7O_2\mathrm{N} + 0.497H_2\mathrm{O} + 0.012H^+ \quad (22)$$

The steady-state biofilm model and the substrate mass balance

In order to employ a model for determining the biofilm kinetics for sulfate reduction and sulfide oxidation, the steady-state mass balances for substrate and active biomass are used with the steady-state biofilm model (Rittmann and McCarty, 2020) to estimate the substrate flux into the biofilm (J_{ss}), substrate levels (S) and biomass growth (X_f).

Steady-state mass balance for substrate

The steady-state mass balance for the rate-limiting substrate in a CMBR is

$$Q(S^0 - S) - J_{ss}aV = 0 \quad (23)$$

where Q is the influent flow rate (m^3/d), S^0 is the influent substrate concentration (mg O_2 eq/L), S is the effluent substrate concentration (mgO_2 eq/L), J_{ss} is the steady-state substrate flux (mgO_2 eq/cm^2-d), a (m^{-1}) is the biofilm-specific surface area, and V is the reactor volume (m^3). The equation can be rearranged to calculate S as given in equation 24 below.

$$S = S^0 - \frac{J_{ss} a V}{Q} \qquad (24)$$

where $\frac{V}{Q}$ can be replaced by the hydraulic retention time Θ, (d), which represents the average time the feed liquid remains in the reactor. Equation 5.7 can then be written as equation 25.

$$S = S^0 - J_{ss} a \Theta \qquad (25)$$

Steady-state mass balance for active biomass

Similarly, the steady-state biofilm mass balance is presented in equation 26 below.

$$Y J_{ss} a V - (b + b_{det}) X_f L_f a V = 0 \qquad (26)$$

where b is the biofilm loss rate (T^{-1}) and b_{det} is the biofilm detachment loss coefficient (T^{-1}). If J_{ss} is known, the biofilm accumulation, $X_f L_f a$ ($M_x L^{-3}$), can then be calculated using equation 27.

$$X_f L_f a = \frac{J_{ss} a}{(b + b_{det})} \qquad (27)$$

The steady-state biofilm model

To calculate J_{ss}, Rittmann & McCarty (2020) presented a pseudo-analytical method using three dimensionless parameters: K*, S* and S_{bmin}* that represent the dimensionless half-maximum saturation constant, the dimensionless liquid substrate concentration S, and the dimensionless minimum substrate concentration, respectively. The K* value is related to the comparison between the external mass transport and the internal utilization of substrate, and the S^*_{bmin} is related to the growth potential of biofilm (Rittmann & McCarty, 2020).

With these parameters, another important parameter S_s* can be obtained by solving equation 28 iteratively.

$$S_S^* = S^* - \frac{tanh\left[\alpha\left(\frac{S_S^*}{S_{bmin}^*}-1\right)^{\beta}\right]\left[2\left(S_S^*-ln(1+S_S^*)\right)\right]^{0.5}}{K^*} \qquad (28)$$

where α and β are coefficients required for solving the equation (Rittmann and McCarty, 2020).

From the calculation of S_s*, the dimensionless flux J* can be calculated using equation 29.

$$J^* = K^*(S^* - S_S^*) \qquad (29)$$

from which J_{ss} can be calculated using equation 30.

$$J = J^*\left(KqX_f D_f\right)^{0.5} \qquad (30)$$

Estimation of biofilm-specific parameters

Table 2 presents the necessary input parameters to implement the model for sulfate reduction and sulfur oxidation kinetics.

Table 2-The required parameters for the steady-state biofilm and mass balance solutions

PARAMETER	EQUATION/SOURCE	$SO_4^{2-} \rightarrow S^{2-}$ by SRB	$S^{2-} \rightarrow S^0$ by SOB
Half-maximum rate concentration, K (mg mgO_2 eq/L)	(Tang et al., 2013), (Xu et al., 2013)	0.5	11
Biofilm loss rate, b (d^{-1})	(Rittmann & McCarty, 2020), (Wang et al., 2010)	0.02	0.05
Biofilm detachment loss coefficient, b_{det} (d^{-1})	Estimated	0.05	0.05
Minimum substrate concentration, S_{bmin} (mg O_2 eq/L)	$K\frac{b+b_{det}}{\mu_{max}-(b+b_{det})}$	0.15	0.54
S^*_{bmin}	$\frac{b+b_{det}}{\mu_{max}-(b+b_{det})}$	0.30	0.048
Active biomass density, X_f (mg_x/cm^3)	(Rittmann & McCarty, 2020)	70	30
Substrate diffusion coefficient in water, D (cm^2/d)	(Mondal et al., 2016)	0.9	0.63
Effective diffusion layer thickness, L (cm)	Estimated	0.015	0.015
Substrate diffusion coefficient in biofilm, D_f (cm^2/d)	0.8D	0.72	0.504
K*	$\frac{D}{L}\left[\frac{K}{q\,X_f\,D_f}\right]^{\frac{1}{2}}$	0.08	0.42
Coefficient for pseudo-analytical solution, α	$1.557-0.4117\tanh[\log_{10}S^*_{bmin}]$	1.75	1.9
Coefficient for pseudo-analytical solution, β	$0.5035-0.0257\tanh[\log_{10}S^*_{bmin}]$	0.53	0.52

Comparing the computed biofilm parameter values for the two processes (sulfate reduction versus sulfide oxidation), the minimum substrate concentration values (S_{bmin}) for both processes are below 1 mg O_2 eq/L. This indicates that both types of bacteria are able to grow under low substrate conditions. The S^*_{bmin} values for both processes are also below one, indicating a high growth potential. However, the growth potential is higher for SOB because the value is well below 1, as compared to the value for SOB. A large difference is observed in the K values, resulting in a large difference in the K* values as well. These values are important to note as the affect the overall output values of the model.

With the above equations and parameter values, the trends of the substrate flux, biofilm density and hydraulic retention time (HRT) for removal levels of 50% and higher were investigated. The influent substrate concentration (S^0) was taken as 1500 mgSO_4^{2-}/L (1000 mg O_2 eq/L), and the specific surface *a* was taken as 800 m^2/m^3 (for commercial scale).

The donor concentrations required and the alkalinity for pH regulation are then determined for each process by using the stoichiometry in equations 21 and 22. The calculations are made based on the stoichiometric ratios of the species involved.

I used MATLAB and Microsoft Excel for computations and RStudio for presentation of the results.

6. RESULTS AND ANALYSIS

The results of running the model provide trends for changes in substrate flux with substrate removal, changes in biofilm density with substrate flux, and the required hydraulic retention time (HRT) for various %-removals.

Trends in Sulfate Reduction

Figure 6 presents the trends of substrate flux, biofilm density, and HRT for a range of sulfate removals obtained from the solution of the steady-state biofilm model and a mass balance with an influent sulfate concentration S^0 = 1000 mg O_2 eq /L. The blue line was obtained from plotting effluent substrate concentrations from S = 500 mg O_2 eq /L (50% removal) to S = 0 mg O_2 eq/L (100% removal) against the substrate flux (J_{ss} in mg O_2 eq/cm^2-d). The red line was obtained from calculating the biofilm accumulation (X_fL_f in mg_x/L) at different values of J_{ss} (obtained for the different effluent substrate concentrations). The green line shows the hydraulic retention time (HRT) required for each substrate removal level from 50% removal to the maximum-achievable removal. Each component of the plot is further analyzed below.

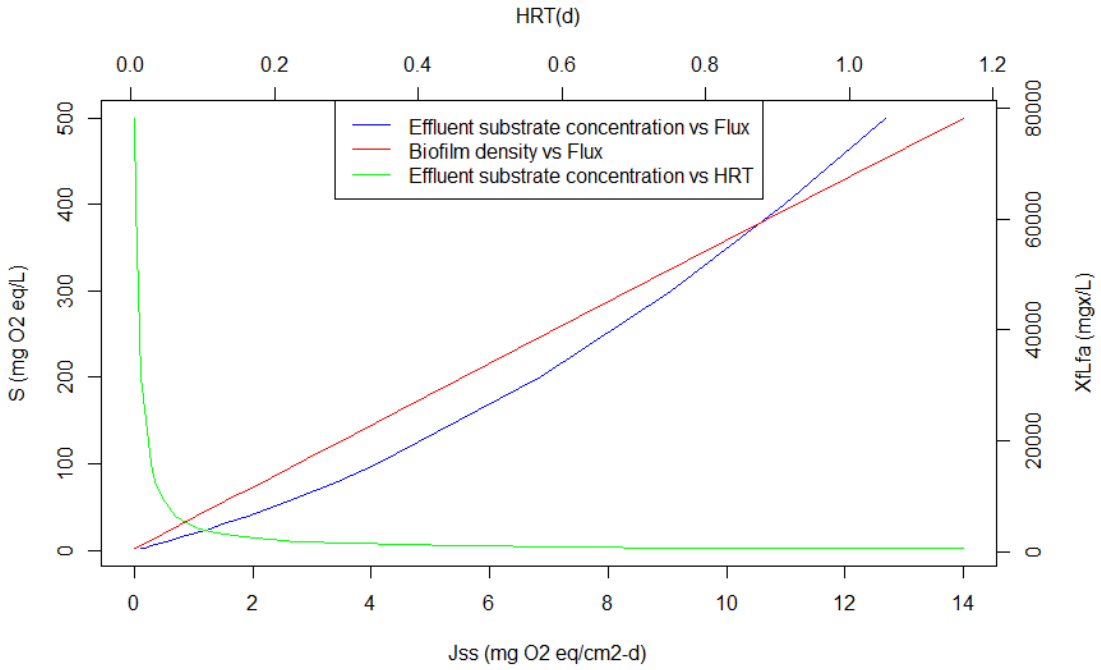

Figure 6 - MBfR performance showing the trends in sulfate effluent concentration (blue and green lines), biofilm accumulation (red line) versus substrate flux and HRT.

Changes in flux and biofilm accumulation with changing substrate removal levels

The results as shown in Figure 7 demonstrates the trend in changes in J_{ss} with changing effluent substrate concentrations and the corresponding change in biofilm accumulation. Figure 7 shows how S and X_fL_fa are related to J_{ss}. J_{ss} is highest (12.7 mgO_2 eq/cm^2-d) at 50% percent removal of S (i.e., S = 500 mg OE/L). J_{ss} is lowest at low S and approaches 0 mgO_2 eq/cm^2-d as S approaches S_{bmin} = 0.15 mg O_2 eq/L. The slope is highest at high S values (between 200 mg O_2 eq /L and 500 mg O_2 eq /L). As S decreases towards S_{bmin}, the changes in J_{ss} with increasing removal levels also smaller, resulting in the non-linear relationship observed. The non-linear response is based on mass transport becoming more significant in controlling substrate removal at high J_{ss} values.

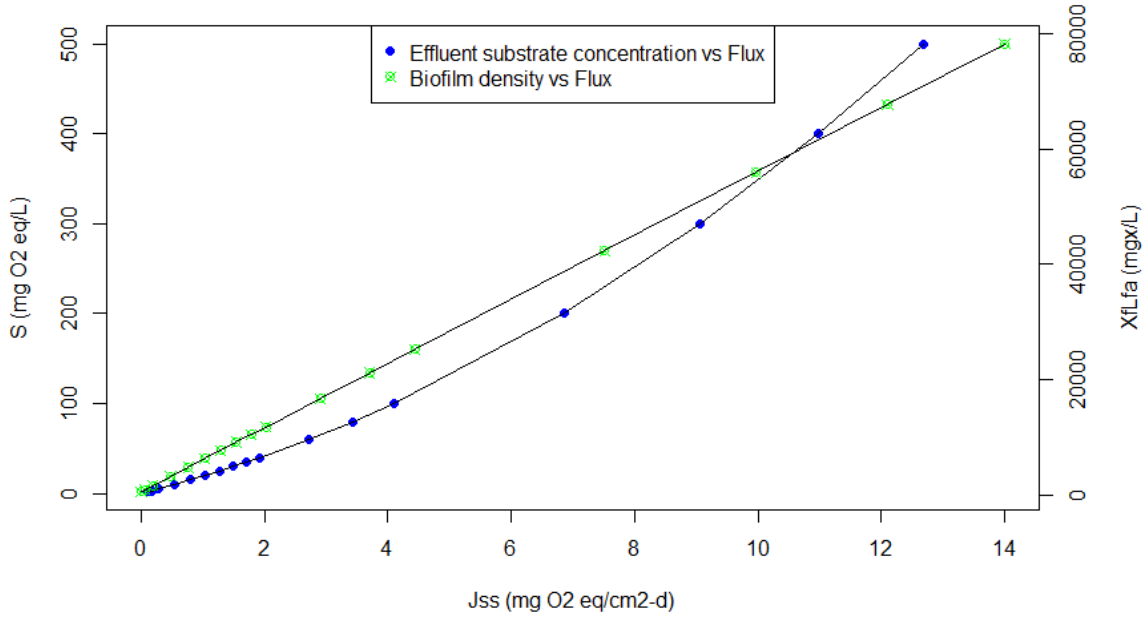

Figure 7- Trends of the change in flux and biofilm accumulation with increasing removal levels for sulfate reduction.

A linear relationship is observed between the substrate flux J_{ss} and the biofilm density $X_f L_f a$. Thick biofilms (equal to about 80,000 mg_x/L in the reactor) are obtained for the least substrate removal considered (50% removal), which is at high J_{ss} value. As J_{ss} decreases, the biofilm density decreases until the value of J_s at S_{bmin}, below which no biofilm is observed, because biofilm loss always exceeds growth (Nerenberg, 2016; Rittmann and McCarty, 2020). The biofilm thickness (L_f) values range between about 1400 µm and 10 µm for removal levels between 50% and 99%. High L_f values correspond to high removal rates (Chen et al., 2017), but too high L_f may result in biofilm detachment (Torresi et al., 2016).

Trend of hydraulic retention time with changing removal levels

Figure 8 shows that higher HRT values are required for higher substrate removal. As the removal levels increases above 98%, significantly higher HRT values are needed for a small increase in % removal level. For example, increasing the removal from 99.5% to 99.7% increases the required HRT from 0.46 d to 0.78 d, while increasing from 99.7% to 99.8% increases the required HRT to 1.16 d due to the decrease in the substrate flux values. From this analysis, an "optimum" removal can be taken as 97.5%, which has an effluent sulfate concentration (S) of 25 mg O_2 eq /L, a flux of 1.26 mg O_2 eq/cm^2-d, and an HRT of ~0.1 d. The biofilm thickness L_f at the selected optimum removal level is 150 µm.

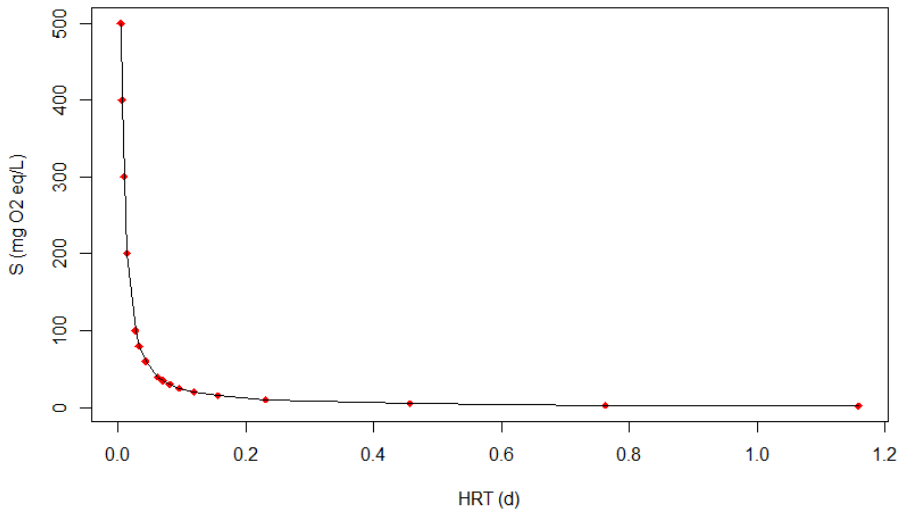

Figure 8 - Trend of required HRT for different effluent substrate concentrations for sulfate reduction.

Trends in Sulfide Oxidation

To do the analysis of the trends of sulfide oxidation, I assume that all of the reduced sulfate is converted into sulfide. Therefore, for the optimum effluent sulfate concentration of 25 mg O_2 eq /L selected, the concentration of the influent for sulfide removal (S^0) is 975 mg O_2 eq /L.

Figure 9 is a graphical representation of the trends of substrate flux, biofilm density and HRT at various sulfate removal levels obtained from the solution of the steady-state biofilm model and the mass balance with an influent sulfate concentration (S^0) = 975 mg O_2 eq /L. Individual trends are discussed below.

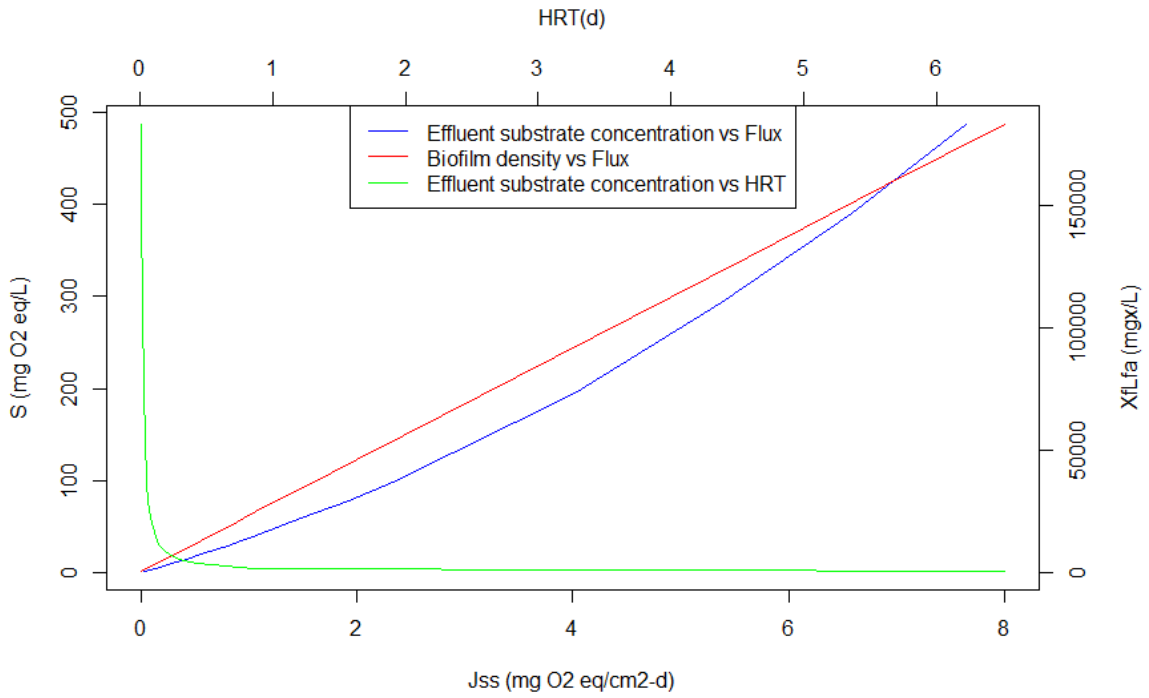

Figure 9 - Reactor performance showing the trends in sulfide removal, biofilm accumulation. and flux for sulfide oxidation in the O_2-MBfR.

The trends are similar to what was obtained for the sulfate reduction present previously. The blue line was obtained from plotting the effluent substrate concentrations from S = 487 mg O_2 eq /L (50% removal) to the maximum achievable removal against the substrate flux (J_{ss}). The red line is obtained from calculating the biofilm density at different values of J_{ss} (obtained at different effluent substrate concentrations). The green line shows the hydraulic retention time (HRT) required for each substrate removal level from 50% removal the maximum achievable removal.

Changes in flux and biofilm accumulation with changing substrate removal levels

The results shown in Figure 10 demonstrate the trend in changes in J_{ss} with changing effluent substrate concentrations and the corresponding change in biofilm accumulation. Similar to the trends of the sulfate reduction, a non-linear relationship is observed between the sulfate removal levels and the substrate flux. However, lower values of substrate flux are observed for the same % removal levels, which can be attributed to the higher half-maximum saturation constant (K) value used in the steady-state biofilm model solution of J_{ss} for sulfide oxidation. J_{ss} is highest (7.64 mgO_2 eq/cm^2-d) at 50% percent removal of S and decreases with increasing substrate removal. J_{ss} is lowest at low S and approaches 0 mgCOD/cm^2-d as S approaches S_{bmin} = 0.54 mg O_2 eq /L.

Again, a linear relationship is observed between the substrate flux J_{ss} and the biofilm density $X_f L_f a$ for sulfide reduction, similar to the trend in Figure 8. Even at the low substrate flux levels, higher values of biofilm accumulation are obtained (about 180000mgCOD_x/L at 50% substrate removal) as compared to the biofilm density values for sulfate reduction. As previously observed, SOB has a higher growth (S^*_{bmin}) potential

as compared to SOB. This is due to a higher yield (Y) for SOB, resulting in a higher maximum specific growth rate and thus the higher biofilm accumulation observed. As J_{ss} decreases, the biofilm density decreases till the value of J_{ss} at S_{bmin} below which no biofilm growth is observed. The biofilm thickness (L_f) values range between about 3000µm and 10µm for removal levels between 50% and 99%.

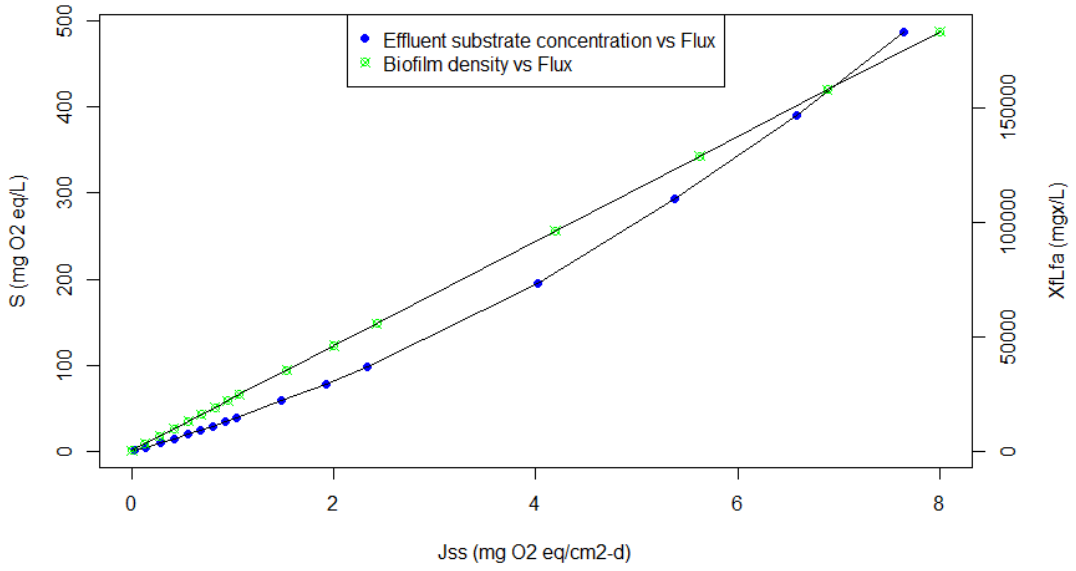

Figure 10 - Trends of the change in flux and biofilm accumulation with increasing removal levels for sulfide oxidation.

Trend of hydraulic retention time with changing removal levels

The values of the HRT begin at 0.008 days for 50% removal and increases steadily with increasing removal. This trend is observed in Figure 11. Similar to the trend observed as the removal rate increases for sulfate reduction, a significant jump in the required HRT is

observed when the effluent substrate concentration is reduced from about 5 mg O_2 eq /L to 1 mg O_2 eq /L (99.5% removal to 99.9% removal). The required HRT increases from 0.9 d to 6.5 d. This is due to the significantly low J_{ss} value of 0.019 mgO_2 eq/cm^2-d at 99.9% removal. T he low J_{ss} values obtained for sulfide removal results in generally higher HRT values when compared to the HRT values required for sulfate reduction for the same removal levels.

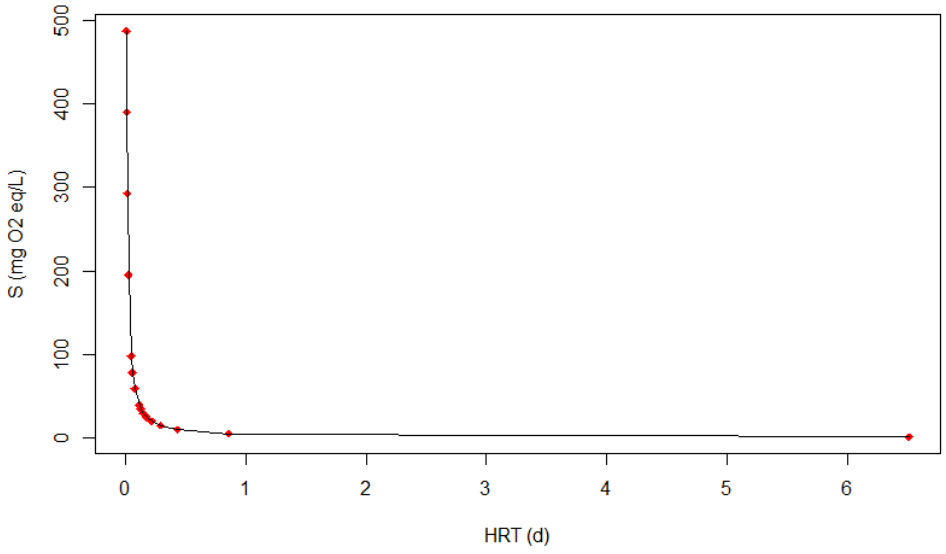

Figure 10-Graph showing the trend of required HRT for different effluent substrate concentrations at increasing percent removal levels for sulfide oxidation.

The optimum sulfide removal is taken to be at 97.5% (S = 24 mg O_2 eq /L) with a required HRT of ~0.2 d. This HRT is about twice that of the sulfate-reducing H_2-MBfR. The HRT for the O_2-MBfR is larger because of the low flux (J_{ss}) values. The large

difference in the K values (that of SOB being about 20 times that of SRB) resulted in the difference in the computed flux values and hence the difference in HRT values.
The biofilm thickness L_f at the selected optimum removal level is about 290 μm.

As indicated previously, these analyses were done assuming sulfate (in the case of sulfate reduction) and sulfide (in the case of sulfide oxidation) are the rate-limiting substrates. Limitation of gases (H_2 and O_2) will cause the bacteria to be outcompeted resulting in reduce sulfate reduction and sulfide oxidation respectively, lower fluxes, lower biofilm accumulation and higher HRT values that observed.

Calculation of Required Donor/Acceptor Deliveries, Elemental Sulfur Produced, Biomass Produced, and Changes in Alkalinity

From the model results of the final effluent substrate concentrations for the two processes, the required H_2-delivery rate for sulfate reduction and O_2-delivery rate for sulfide oxidation can be calculated from stoichiometry using equations 21 and 22. The products for each process and the biomass produced also are estimated. All rates are expressed as a concentration in the wastewater flow.

Table 3 presents the results obtained from the calculations for 97.5% removal of sulfate, and Table 4 is for 97.5% removal of sulfide.

Table 3-Calculated values of required H_2 concentration, sulfide produced, biomass produced, and alkalinity generated for sulfate reduction.

Sulfate removed	487.5 mgS/L
Required H_2 (donor) concentration	122 mg H_2/L
CO_2 demand	70 mg/L

Total alkalinity	1520 mg/L as $CaCO_3$
Sulfide produced	487.5 mgS/L
Biomass produced	36 mg VSS/L

Table 4-Calculated values of required O_2 concentration, elemental sulfur produced, biomass produced, and alkalinity generated for sulfide oxidation.

Sulfide removed	475 mgS/L
Required O_2 (acceptor) concentration	95 mg O_2/L
CO_2 demand	81 mg/L
Total alkalinity	18 mg/L as $CaCO_3$
Elemental sulfur produced	475 mg S/L
Biomass produced	41 mg VSS/L

The CO_2 demand is higher for the sulfide oxidizing MBfR as compared to that for the sulfate-reduction MBfR. This is as a result of the difference in stoichiometric coefficients for CO_2 according to equations 21 and 22.

Comparing the values of biomass production of SRB and SOB, a higher value is observed for SOB, due to a higher portion of electrons transferred for cell synthesis (f_s^o) according to the energetics of sulfide oxidation, resulting in a higher stoichiometric coefficient of biomass ($C_5H_7O_2N$) from equations 21 and 22 (0.0025 for SRB and 0.012 for SOB).

For sulfide oxidation, a higher amount of elemental sulfur (about 10 times more) is produced than biomass. This indicates that the effluent from the sulfide-oxidizing bacteria must contain elemental sulfur. This observation raises questions concerning the collection of the elemental sulfur produced. The solid elemental sulfur may be suspended as colloids in the effluent or bound up in the biofilms. Certain methods used for removal of elemental sulfur from biological sulfate removal systems include filtration, example by the use of a vacuum filter (Halfyard & Hawboldt, 2011). The precipitates also can be separated and removed by centrifugation (Tian et al., 2019) or through gravity sedimentation (Cai et al., 2017). If bound in the biofilm, the elemental sulfur may adversely affect growth of the biofilm and subsequent substrate removal in the O_2-MBfR.

Similarly, in the H_2-MBfR, the presence of metal impurities such as iron, copper, and zinc in phosphogypsum may lead to metal-sulfide precipitation. The metallic sulfides may lead to the inhibition of SRB (Zhang et al., 2009) and may even be toxic when present in high concentrations (Utgikar et al., 2002). Also, the solids may be caught up in the membranes, blocking H_2 delivery and thus affecting biofilm growth.

7. SUMMARY AND CONCLUSION

The MBfR should enables high removal of sulfate and recovery of sulfur from phosphate mining wastewater. The steady-state biofilm model is a useful tool in predicting the performance of MBfR in sulfate removal and sulfide oxidation by SRB and SOB, respectively. The modeling suggests that relatively short HRTs are possible for a

commercial-scale MBfR: 0.1 and 0.2 d. This work confirmed lower substrate fluxes and higher biofilm growth for SOB over SRB for the same removal level (97.5%). The model also helps determine the required additions, such as H_2 for sulfate reduction and O_2 for sulfide oxidation, as well as alkalinity or acidity for pH control.

Suggested areas of further research include better definition of microbial parameters for SOB and SRB, especially the determination of the K value, as the magnitude of the values have a significant effect on the computed flux (J_{ss}) values.

As previously stated, other microorganisms present in the reactor, such as methanogens and homoacetogens in the H_2-based MBfR, may compete with the SRB for substrate utilization. Therefore, the subject of the effects of the growth of the other groups of microorganisms on substrate removal is another area of suggested investigation. Furthermore, the production of extra polymeric substances (EPS) and soluble microbial products (SMP) due to biofilm formation, and the use of these products by heterotrophs present in the system should be investigated.

Finally, the recovery of the elemental sulfur produced is a critical topic to be considered. The most efficient methods to recover the sulfur solids for use after they have been produced in the O_2-MBfR should be further investigated.

REFERENCES

A report prepared by the National Mining Association. (2016). https://nma.org/wp-content/uploads/2016/09/Economic-Contributions-of-Mining-in-2015-Update-final.pdf

Adhikari, K., Sadhu, K., Chakroborty, B., & Gangopadhyay, A. (2013). *Effect of Mining on Geochemistry of Groundwater in Permo-carboniferous Gondwana Coalfields: Raniganj Basin, India* (Vol. 82).

Advanced Fluid Dynamics. (2012). In *Advanced Fluid Dynamics*. https://doi.org/10.5772/1520

Arne Alphenaar, P., Visser, A., & Lettinga, G. (1993). The effect of liquid upward velocity and hydraulic retention time on granulation in UASB reactors treating wastewater with a high sulphate content. *Bioresource Technology*, *43*(3), 249–258. https://doi.org/10.1016/0960-8524(93)90038-D

Backer, L. C. (2000). Assessing the acute gastrointestinal effects of ingesting naturally occurring, high levels of sulfate in drinking water. In *Critical Reviews in Clinical Laboratory Sciences* (Vol. 37, Issue 4, pp. 389–400). CRC Press LLC. https://doi.org/10.1080/10408360091174259

Barton, L. L. (Ed.). (1995). *Sulfate-Reducing Bacteria*. Springer US. https://doi.org/10.1007/978-1-4899-1582-5

Barton, L. L., & Fauque, G. D. (2009). Chapter 2 Biochemistry, Physiology and Biotechnology of Sulfate-Reducing Bacteria. In *Advances in Applied Microbiology* (Vol. 68, pp. 41–98). Academic Press. https://doi.org/10.1016/S0065-2164(09)01202-7

Benatti, C. T., Tavares, C. R. G., & Lenzi, E. (2009). Sulfate removal from waste chemicals by precipitation. *Journal of Environmental Management*, *90*(1), 504–511. https://doi.org/10.1016/j.jenvman.2007.12.006

Bologo, V., Maree, J. P., & Carlsson, F. (2012). Application of magnesium hydroxide and barium hydroxide for the removal of metals and sulphate from mine water. *Water SA*, *38*(1), 23–28. https://doi.org/10.4314/wsa.v38i1.4

Catalano S., Palazzolo J., Robertson M., Wesorick S., Nalbandian A., M. K. (2018). *Visual Encyclopedia of Chemical Engineering*. College of Engineering Chemical Engineering University of Michigan. https://encyclopedia.che.engin.umich.edu/Pages/Reactors/PBR/PBR.html

Chao, Y. M., & Liang, T. M. (2008). A feasibility study of industrial wastewater recovery

using electrodialysis reversal. *Desalination*, *221*(1–3), 433–439. https://doi.org/10.1016/j.desal.2007.04.065

Chraiti, R., Raddaoui, M., & Hafiane, A. (2016). Effluent Water Quality at Phosphate Mines in M'Dhilla, Tunisia and its Potential Environmental Effects. *Mine Water and the Environment*, *35*(4), 462–468. https://doi.org/10.1007/s10230-016-0400-x

Csavina, J., Landázuri, A., Wonaschütz, A., Rine, K., Rheinheimer, P., Barbaris, B., Conant, W., Sáez, A. E., & Betterton, E. A. (2011). Metal and metalloid contaminants in atmospheric aerosols from mining operations. *Water, Air, and Soil Pollution*, *221*(1–4), 145–157. https://doi.org/10.1007/s11270-011-0777-x

Cuci, Y., & Taşkın, E. G. (2020). Simultaneous removal of nitrate and pesticide endo-sulfan in groundwater using membrane biofilm reactor. *Journal of Environmental Biology*, *41*(2(SI)), 351–357. https://doi.org/10.22438/jeb/41/2(si)/jeb-11

Czerewko, M. A., Cripps, J. C., Reid, J. M., & Duffell, C. G. (2003). Sulfur species in geological materials - Sources and quantification. *Cement and Concrete Composites*, *25*(7), 657–671. https://doi.org/10.1016/S0958-9465(02)00066-5

Dar, S. A., Kleerebezem, R., Stams, A. J. M., Kuenen, J. G., & Muyzer, G. (2008). Competition and coexistence of sulfate-reducing bacteria, acetogens and methanogens in a lab-scale anaerobic bioreactor as affected by changing substrate to sulfate ratio. *Applied Microbiology and Biotechnology*, *78*(6), 1045–1055. https://doi.org/10.1007/s00253-008-1391-8

DeYoung, J. H., Sutphin, D. M., & Cannon, W. F. (1984). International strategic minerals inventory summary report - manganese. In *US Geological Survey Circular: Vol. 930 J*.

Dissanayake, C. B., & Chandrajith, R. (2009). Phosphate Mineral Fertilizers, trace metals and human health. *Journal of the National Science Foundation of Sri Lanka*, *37*(3), 153–165. https://doi.org/10.4038/jnsfsr.v37i3.1219

Dolla, A., Fournier, M., & Dermoun, Z. (2006). Oxygen defense in sulfate-reducing bacteria. In *Journal of Biotechnology* (Vol. 126, Issue 1, pp. 87–100). Elsevier. https://doi.org/10.1016/j.jbiotec.2006.03.041

Duruibe, J. O., Ogwuegbu, M. O. C., & Egwurugwu. (2007). Heavy metal pollution and human biotoxic effects. In *International Journal of Physical Sciences* (Vol. 2, Issue 5). http://www.academicjournals.org/IJPS

EPA. (2016). *Mineral Mining and Processing Effluent*. https://www.epa.gov/eg/mineral-mining-and-processing-effluent-guidelines

Fischer, K. M., Batstone, D. J., van Loosdrecht, M. C. M., & Picioreanu, C. (2015). A

mathematical model for electrochemically active filamentous sulfide-oxidizing bacteria. *Bioelectrochemistry*, *102*, 10–20. https://doi.org/10.1016/j.bioelechem.2014.11.002

Gibson, G. R. (1990). Physiology and ecology of the sulphate-reducing bacteria. *Journal of Applied Bacteriology*, *69*(6), 769–797. https://doi.org/10.1111/j.1365-2672.1990.tb01575.x

Hakkou, R., Benzaazoua, M., & Bussière, B. (2016). Valorization of Phosphate Waste Rocks and Sludge from the Moroccan Phosphate Mines: Challenges and Perspectives. *Procedia Engineering*, *138*, 110–118. https://doi.org/10.1016/j.proeng.2016.02.068

Heizer, W. D., Sandler, R. S., Seal, E., Murray, S. C., Busby, M. G., Schliebe, B. G., & Pusek, S. N. (1997). Intestinal effects of sulfate in drinking water on normal human subjects. *Digestive Diseases and Sciences*, *42*(5), 1055–1061. https://doi.org/10.1023/A:1018801522760

Hong, Y., & Valix, M. (2014). Bioleaching of electronic waste using acidophilic sulfur oxidising bacteria. *Journal of Cleaner Production*, *65*, 465–472. https://doi.org/10.1016/j.jclepro.2013.08.043

Jiries, A., El-Hasan, T., Al-Hweiti, M., & Seiler, K. P. (2004). Evaluation of the effluent water quality produced at phosphate mines in Central Jordan. *Mine Water and the Environment*, *23*(3), 133–137. https://doi.org/10.1007/s10230-004-0053-z

Kaksonen, A. H., Plumb, J. J., Robertson, W. J., Riekkola-Vanhanen, M., Franzmann, P. D., & Puhakka, J. A. (2006). The performance, kinetics and microbiology of sulfidogenic fluidized-bed treatment of acidic metal- and sulfate-containing wastewater. *Hydrometallurgy*, *83*(1–4), 204–213. https://doi.org/10.1016/j.hydromet.2006.03.025

Khanal, S. K., & Huang, J.-C. (2005). Effect of High Influent Sulfate on Anaerobic Wastewater Treatment. *Water Environment Research*, *77*(7), 3037–3046. https://doi.org/10.2175/106143005x73929

Langner, H. W., Greene, E., Domenech, R., & Staats, M. F. (2012). Mercury and other mining-related contaminants in ospreys along the upper Clark Fork River, Montana, USA. *Archives of Environmental Contamination and Toxicology*, *62*(4), 681–695. https://doi.org/10.1007/s00244-011-9732-5

Lens, P. N. L., Visser, A., Janssen, A. J. H., Hulshoff Pol, L. W., & Lettinga, G. (1998). Biotechnological treatment of sulfate-rich wastewaters. In *Critical Reviews in Environmental Science and Technology* (Vol. 28, Issue 1, pp. 41–88). Taylor & Francis. https://doi.org/10.1080/10643389891254160

Liamleam, W., & Annachhatre, A. P. (2007). Electron donors for biological sulfate reduction. *Biotechnology Advances*, *25*(5), 452–463. https://doi.org/10.1016/j.biotechadv.2007.05.002

Liang, F., Xiao, Y., & Zhao, F. (2013). Effect of pH on sulfate removal from wastewater using a bioelectrochemical system. *Chemical Engineering Journal*, *218*, 147–153. https://doi.org/10.1016/j.cej.2012.12.021

Liu, H., Zhang, Q., Li, V., Su, H., & Gu, C. (2017). Durability study on engineered cementitious composites (ECC) under sulfate and chloride environment. *Construction and Building Materials*, *133*, 171–181. https://doi.org/10.1016/j.conbuildmat.2016.12.074

Liu, W. X., Coveney, R. M., & Chen, J. L. (2003). Environmental quality assessment on a river system polluted by mining activities. In *Applied Geochemistry* (Vol. 18, Issue 5). https://doi.org/10.1016/S0883-2927(02)00155-5

Liu, Z., Zhou, C., Ontiveros-Valencia, A., Luo, Y. H., Long, M., Xu, H., & Rittmann, B. E. (2018). Accurate O 2 delivery enabled benzene biodegradation through aerobic activation followed by denitrification-coupled mineralization. *Biotechnology and Bioengineering*, *115*(8), 1988–1999. https://doi.org/10.1002/bit.26712

Macías, F., Caraballo, M. A., Nieto, J. M., Rötting, T. S., & Ayora, C. (2012). Natural pretreatment and passive remediation of highly polluted acid mine drainage. *Journal of Environmental Management*, *104*, 93–100. https://doi.org/10.1016/j.jenvman.2012.03.027

Macías, F., Caraballo, M. A., Rötting, T. S., Pérez-López, R., Nieto, M., & Ayora, C. (2012). *From highly polluted Zn-rich acid mine drainage to non-metallic waters: Implementation of a multi-step alkaline passive treatment system to remediate metal pollution*. https://doi.org/10.1016/j.scitotenv.2012.06.084

Macklin, M. G., Brewer, P. A., Hudson-Edwards, K. A., Bird, G., Coulthard, T. J., Dennis, I. A., Lechler, P. J., Miller, J. R., & Turner, J. N. (2006). A geomorphological approach to the management of rivers contaminated by metal mining. *Geomorphology*, *79*(3–4), 423–447. https://doi.org/10.1016/j.geomorph.2006.06.024

Meulepas, R. J. W., Stams, A. J. M., & Lens, P. N. L. (2010). Biotechnological aspects of sulfate reduction with methane as electron donor. *Reviews in Environmental Science and Biotechnology*, *9*(1), 59–78. https://doi.org/10.1007/s11157-010-9193-8

Moreno, P., Ingeniería, F. De, & Portales, U. D. (2009). *Environmental Impact and Toxicology of Sulphate*. *December 2016*, 1–10.

https://www.researchgate.net/publication/282293143

Moutsatsou, A., Gregou, M., Matsas, D., & Protonotarios, V. (2006). Washing as a remediation technology applicable in soils heavily polluted by mining-metallurgical activities. *Chemosphere, 63*(10), 1632–1640. https://doi.org/10.1016/j.chemosphere.2005.10.015

Noller, B. N. (1991). Non-radiological contaminants from uranium mining and milling at Ranger, Jabiru, Northern Territory, Australia. *Environmental Monitoring and Assessment, 19*(1–3), 383–400. https://doi.org/10.1007/BF00401327

Ontiveros-Valencia, A., Zhou, C., Zhao, H. P., Krajmalnik-Brown, R., Tang, Y., & Rittmann, B. E. (2018). Managing microbial communities in membrane biofilm reactors. *Applied Microbiology and Biotechnology*, *102*(21), 9003–9014. https://doi.org/10.1007/s00253-018-9293-x

Ontiveros-Valencia, Aura, Penton, C. R., Krajmalnik-Brown, R., & Rittmann, B. E. (2016). Hydrogen-fed biofilm reactors reducing selenate and sulfate: Community structure and capture of elemental selenium within the biofilm. *Biotechnology and Bioengineering*, *113*(8), 1736–1744. https://doi.org/10.1002/bit.25945

Ontiveros-Valencia, Aura, Tang, Y., Krajmalnik-Brown, R., & Rittmann, B. E. (2014). Managing the interactions between sulfate- and perchlorate-reducing bacteria when using hydrogen-fed biofilms to treat a groundwater with a high perchlorate concentration. *Water Research*, *55*, 215–224. https://doi.org/10.1016/j.watres.2014.02.020

Ontiveros-Valencia, Aura, Ziv-El, M., Zhao, H. P., Feng, L., Rittmann, B. E., & Krajmalnik-Brown, R. (2012). Interactions between nitrate-reducing and sulfate-reducing bacteria coexisting in a hydrogen-fed biofilm. *Environmental Science and Technology*, *46*(20), 11289–11298. https://doi.org/10.1021/es302370t

Orris, G. J., & Chernoff, C. B. (2004). Chapter 20 Review of world sedimentary phosphate deposits and occurrences. *Handbook of Exploration and Environmental Geochemistry*, *8*, 559–573. https://doi.org/10.1016/S1874-2734(04)80022-6

Othman, I., & Al-Masri, M. S. (2007). Impact of phosphate industry on the environment: A case study. *Applied Radiation and Isotopes, 65*(1), 131–141. https://doi.org/10.1016/j.apradiso.2006.06.014

Oztemur, G., Teksoy Basaran, S., Tayran, Z., & Sahinkaya, E. (2020). Fluidized bed membrane bioreactor achieves high sulfate reduction and filtration performances at moderate temperatures. *Chemosphere, 252*. https://doi.org/10.1016/j.chemosphere.2020.126587

Papirio, S., Villa-Gomez, D. K., Esposito, G., Pirozzi, F., & Lens, P. N. L. (2013). Acid

mine drainage treatment in fluidized-bed bioreactors by sulfate-reducing bacteria: A critical review. In *Critical Reviews in Environmental Science and Technology* (Vol. 43, Issue 23, pp. 2545–2580). https://doi.org/10.1080/10643389.2012.694328

Petavratzi, E., Kingman, S., & Lowndes, I. (2005). *Particulates from mining operations: A review of sources, effects and regulations*. https://doi.org/10.1016/j.mineng.2005.06.017

Pokorna, D., & Zabranska, J. (2015). Sulfur-oxidizing bacteria in environmental technology. In *Biotechnology Advances* (Vol. 33, Issue 6, pp. 1246–1259). Elsevier Inc. https://doi.org/10.1016/j.biotechadv.2015.02.007

Qian, Z., Tianwei, H., Mackey, H. R., van Loosdrecht, M. C. M., & Guanghao, C. (2019a). Recent advances in dissimilatory sulfate reduction: From metabolic study to application. In *Water Research* (Vol. 150, pp. 162–181). Elsevier Ltd. https://doi.org/10.1016/j.watres.2018.11.018

Qian, Z., Tianwei, H., Mackey, H. R., van Loosdrecht, M. C. M., & Guanghao, C. (2019b). Recent advances in dissimilatory sulfate reduction: From metabolic study to application. In *Water Research* (Vol. 150, pp. 162–181). Elsevier Ltd. https://doi.org/10.1016/j.watres.2018.11.018

Reta, G., Dong, X., Li, Z., Su, B., Hu, X., Bo, H., Yu, D., Wan, H., Liu, J., Li, Y., Xu, G., Wang, K., & Xu, S. (2018). Environmental impact of phosphate mining and beneficiation: review. *International Journal of Hydrology*, *2*(4). https://doi.org/10.15406/ijh.2018.02.00106

Reta, G. L., Dong, X., Su, B., Hu, X., Bo, H., Wan, H., Liu, J., Li, Y., Peng, T., Ma, H., Wang, K., & Xu, S. (2019). The Influence of Large Scale Phosphate Mining on the Water Quality of the Huang He River Basin in China: Dominant Pollutants and Spatial Distributions. *Mine Water and the Environment*, *38*(2), 366–377. https://doi.org/10.1007/s10230-019-00604-6

Rittmann, B. E. (2011). The membrane biofilm reactor is a versatile platform for water and wastewater treatment. *Environmental Engineering Research*, *16*(4), 157–175. https://doi.org/10.4491/eer.2007.12.4.157

Rittmann, B., & Mccarty, P. (2020). Environmental Biotechnology: Principles and Applications, 2nd ed., McGraw-Hill Book Co., New York.

Rowan, F. E., Docherty, N. G., Coffey, J. C., & O'Connell, P. R. (2009). Sulphate-reducing bacteria and hydrogen sulphide in the aetiology of ulcerative colitis. In *British Journal of Surgery* (Vol. 96, Issue 2, pp. 151–158). https://doi.org/10.1002/bjs.6454

Runtti, H., Tolonen, E. T., Tuomikoski, S., Luukkonen, T., & Lassi, U. (2018a). How to

tackle the stringent sulfate removal requirements in mine water treatment—A review of potential methods. In *Environmental Research*. https://doi.org/10.1016/j.envres.2018.07.018

Runtti, H., Tolonen, E. T., Tuomikoski, S., Luukkonen, T., & Lassi, U. (2018b). How to tackle the stringent sulfate removal requirements in mine water treatment—A review of potential methods. In *Environmental Research* (Vol. 167, pp. 207–222). https://doi.org/10.1016/j.envres.2018.07.018

Santos, A. A., Venceslau, S. S., Grein, F., Leavitt, W. D., Dahl, C., Johnston, D. T., & Pereira, I. A. C. (2015). A protein trisulfide couples dissimilatory sulfate reduction to energy conservation. *Science*, *350*(6267), 1541–1545. https://doi.org/10.1126/science.aad3558

Schwarz, A., Suárez, J. I., Aybar, M., Nancucheo, I., Martínez, P., & Rittmann, B. E. (2020). A membrane-biofilm system for sulfate conversion to elemental sulfur in mining-influenced waters. *Science of the Total Environment*, *740*. https://doi.org/10.1016/j.scitotenv.2020.140088

Serbula, S. M., Milosavljevic, J. S., Radojevic, A. A., Kalinovic, J. V., & Kalinovic, T. S. (2017). Extreme air pollution with contaminants originating from the mining–metallurgical processes. *Science of the Total Environment*, *586*, 1066–1075. https://doi.org/10.1016/j.scitotenv.2017.02.091

Silva, A. J., Varesche, M. B., Foresti, E., & Zaiat, M. (2002). Sulphate removal from industrial wastewater using a packed-bed anaerobic reactor. *Process Biochemistry*, *37*(9), 927–935. https://doi.org/10.1016/S0032-9592(01)00297-7

Sims, D. B. (2011). *Fate of Contaminants at an Abandoned Mining site in an Arid Environment*. *May*, 189. https://doi.org/10.13140/RG.2.2.26844.23683

Sousa, J. R., Silveira, C. M., Fontes, P., Roma-Rodrigues, C., Fernandes, A. R., Van Driessche, G., Devreese, B., Moura, I., Moura, J. J. G., & Almeida, M. G. (2017). Understanding the response of Desulfovibrio desulfuricans ATCC 27774 to the electron acceptors nitrate and sulfate - biosynthetic costs modulate substrate selection. *Biochimica et Biophysica Acta - Proteins and Proteomics*, *1865*(11), 1455–1469. https://doi.org/10.1016/j.bbapap.2017.07.021

Sun, X., Li, B., Han, F., Xiao, E., Wang, Q., Xiao, T., & Sun, W. (2019). Vegetation type impacts microbial interaction with antimony contaminants in a mining-contaminated soil environment. *Environmental Pollution*, *252*, 1872–1881. https://doi.org/10.1016/j.envpol.2019.06.070

Tait, S., Clarke, W. P., Keller, J., & Batstone, D. J. (2009). Removal of sulfate from high-strength wastewater by crystallisation. *Water Research*, *43*(3), 762–772. https://doi.org/10.1016/j.watres.2008.11.008

Tayibi, H., Choura, M., López, F. A., Alguacil, F. J., & López-Delgado, A. (2009). Environmental impact and management of phosphogypsum. In *Journal of Environmental Management* (Vol. 90, Issue 8, pp. 2377–2386). Academic Press. https://doi.org/10.1016/j.jenvman.2009.03.007

Wang, C., Hu, X., Chen, M. L., & Wu, Y. H. (2005). Total concentrations and fractions of Cd, Cr, Pb, Cu, Ni and Zn in sewage sludge from municipal and industrial wastewater treatment plants. *Journal of Hazardous Materials*, *119*(1–3), 245–249. https://doi.org/10.1016/j.jhazmat.2004.11.023

Wycisk, P., Weiss, H., Kaschl, A., Heidrich, S., & Sommerwerk, K. (2003). Groundwater pollution and remediation options for multi-source contaminated aquifers (Bitterfeld/Wolfen, Germany). *Toxicology Letters*, *140–141*, 343–351. https://doi.org/10.1016/S0378-4274(03)00031-6

Zhang, P. (2014). Comprehensive recovery and sustainable development of phosphate resources. *Procedia Engineering*, *83*, 37–51. https://doi.org/10.1016/j.proeng.2014.09.010

Zhao, C., Gupta, V. V. S. R., Degryse, F., & McLaughlin, M. J. (2017). Abundance and diversity of sulphur-oxidising bacteria and their role in oxidising elemental sulphur in cropping soils. *Biology and Fertility of Soils*, *53*(2), 159–169. https://doi.org/10.1007/s00374-016-1162-0

Zhao, H. P., Ilhan, Z. E., Ontiveros-Valencia, A., Tang, Y., Rittmann, B. E., & Krajmalnik-Brown, R. (2013). Effects of multiple electron acceptors on microbial interactions in a hydrogen-based biofilm. *Environmental Science and Technology*, *47*(13), 7396–7403. https://doi.org/10.1021/es401310j

Zhao, H. P., Van Ginkel, S., Tang, Y., Kang, D. W., Rittmann, B., & Krajmalnik-Brown, R. (2011). Interactions between perchlorate and nitrate reductions in the biofilm of a hydrogen-based membrane biofilm reactor. *Environmental Science and Technology*, *45*(23), 10155–10162. https://doi.org/10.1021/es202569b

Zhou, C., Ontiveros-Valencia, A., Nerenberg, R., Tang, Y., Friese, D., Krajmalnik-Brown, R., & Rittmann, B. E. (2019). Hydrogenotrophic microbial reduction of oxyanions with the membrane biofilm reactor. *Frontiers in Microbiology*, *9*(January), 1–14. https://doi.org/10.3389/fmicb.2018.03268

Zitomer, D. H., & Shrout, J. D. (2000). High-Sulfate, High-Chemical Oxygen Demand Wastewater Treatment Using Aerated Methanogenic Fluidized Beds. *Water Environment Research*, *72*(1), 90–97. https://doi.org/10.2175/106143000x137158